Carbon Nanotube Assisted Formation of Sub-50 nm Polymeric Nano-structures

By

Chia-Hua Lee

B.S. Chemical Engineering
National Taiwan University, 2003

M.S. Polymer Science and Engineering
National Taiwan University, 2005

Submitted to the Department of Materials Science and Engineering
in Partial Fulfillment of the Requirement for the Degree of

Master of Science

at the

Massachusetts Institute of Technology

September 2008

Signature of Author: _____
Department of Materials Science and Engineering
August 6th, 2008

Certified by: _____
Karen K. Gleason
Alexander and I. Michael Kasser Professor of Chemical Engineering
Thesis Advisor

Certified by: _____
Silvija Gradečak
Merton C. Flemings Assistant Professor of Materials Science and Engineering
Thesis Reader

Accepted by: _____
Samuel M. Allen
POSCO Professor of Physical Metallurgy
Chair, Departmental Committee on Graduate Students

Carbon Nanotube Assisted Formation of Sub-50 nm Polymeric Nano-structures

By

Chia-Hua Lee

Submitted to the Department of Materials Science and Engineering
on August 6th, 2008 in partial fulfillment of the
requirement for the Degree of Master of Science in
Materials Science and Engineering

Abstract

A novel processing method was developed for sub-50 nm structures by integrating quantum dots (QDs) on patterned polymer substrates. Poly(styrene-*alt*-maleic anhydride) (PSMa) was prepared by the initiated chemical vapor deposition (iCVD) method, an alternative to spin-on deposition. The sub-50 nm PSMa polymer patterns were prepared by low energy oxygen plasma etching by using CNTs as the masks. The water soluble, amine-functionalized QDs underwent the nucleophilic acyl substitution reaction with the PSMa containing anhydride functional groups. This integration method is use to incorporate high performance QDs on inexpensive, lightweight flexible substrate.

Thesis Supervisor: Karen K. Gleason

Title: Alexander and I. Michael Kasser Professor of Chemical Engineering

Table of Contents

Chapter 1 Introduction 1
1.1 Objective 1
1.2 Initiated Chemical Vapor Deposition (iCVD) 2
1.3 Lithographic Techniques 3
1.3.1 Photolithography 3
1.3.2 Electron Beam Lithography (E-beam Lithography) 4
1.3.3 Non-conventional Lithography 5
1.4 Polymer Patterns Fabricated by Using Carbon Nanotubes as Etching Masks 5
1.5 Quantum Dots – Properties and Application 6
1.6 Carbon Nanotubes Alignment 8

Chapter 2 Experimental 10
2.1 Initiated Chemical Vapor Deposition (iCVD) 10
2.2 Functional Polymer, PSMa Synthesized via iCVD 11
2.3 Polymer Patterns and Polymer/Quantum Dots Patterns 12
2.3 CNTs Alignment Work 14
2.4 Instrumentation 15
1) Initiated Chemical Vapor Deposition (iCVD) Chamber and Accessories 15
2) Fourier transform infrared spectroscopy (FTIR) 16
3) Variable Angle Spectroscopic Ellipsometry (VASE) 16
4) Scanning Electron Microscope (SEM) 16
5) UV-Visible Measurement 17
6) Fluorescence Microscope 17
7) Optical Microscope 17
8) O_2 Plasma Chamber 17
9) Atomic Force Microscope (AFM) 18

Chapter 3 Results and Discussion 19

3.1 Deposition of Poly(styrene-alt-maleic anhydirde) via iCVD 19
3.2 Polymer Patterns Fabricated by Using Carbon Nanotubes as Etching Masks 20
3.3 Polymer Patterns Incorporated with Quantum Dots 25
3.4 Carbon Nanotubes Alignment Work 28

Chapter 4 Summary 35

Chapter 5 Future Work 37

Reference 39

List of Figures

Figure1. Illustration of the initiated chemical vapor deposition (iCVD) chamber
Figure2. Structure of monomers and polymer
Figure3. Approaches for fabricating polymer patterns on the silicon wafer: (a) Spin casting of CNT masks on the iCVD PSMa polymer thin film; (b) Oxygen plasma etching; (c) Removal of CNT masks; (d) Quantum dots incorporation.
Figure4. (a) Chemical structure of the ink, 1-hexadecylamine (HDA). (b) Schematics of microcontact printing using HAD as the inks.
Figure5. FTIR spectrum of the anhydride functionality of poly(styrene-alt-maleic anhydride) thin film used in this thesis
Figure6. SEM image of the polymer substrate after spin-casting of carbon nanotubes and etching of polymer
Figure7. SEM images of the polymer substrate after etching and partial removal of the CNTs. (a) etching time was 30 sec; (b) etching time was 50 sec.
Figure8. SEM image of the polymer substrate after etching and removal of the CNTs. (a) etching time was 20 sec; (b) etching time was 30 sec; (c) etching time was 50 sec; (d) etching time was 60 sec
Figure9. Relation between the functional polymer pattern sizes and the etching time.
Figure10. SEM image of the quantum dots decorating a polymer pattern
Figure11. UV spectra of (a) functional polymer, PSMa, (b) quantum dots, CdSe, and (c) quantum dots incorporated functional polymer.
Figure12. Fluorescent microscope images of (a) functional polymer thin film, PSMa, (b) quantum dots (CdSe) incorporated blanket functional polymer thin film, and **(c)** quantum dots (CdSe) incorporated functional polymer patterns.
Figure13. Optical microscopic images of the stamp.
Figure14. Schematic representation of the approaches to align the carbon nanotubes on the silicon wafer.
Figure15. AFM image of the substrate after depositing carbon nanotubes dispersed by surfactants and before rinsing the sample with a copious amount of DI water.
Figure16. AFM images of oriented carbon nanotubes in polar area. (a) height image and (b) phase image.
Figure17. AFM images of oriented carbon nanotubes in polar area. (a) height image and (b) phase image.
Figure18. AFM images of oriented carbon nanotubes in polar area. (a) height image and (b) phase image.
Figure19. Illustration of parallel metal-semiconductor junctions.

List of Schemes

Scheme1. Proposed reaction scheme for the synthesis of covalently attached CdSe quantum dots on functional polymer, PSMa, using amine functionalized quantum dots.

Chapter 1 Introduction

1.1 Objective

The principle objective of this project is to develop a new approach to pattern functional organic films deposited by initiated chemical vapor deposition (iCVD) with sub-50 nm resolution. A second object is to demonstrate the utility of the patterned iCVD layers for tethering nanoparticles.

The iCVD process is an all-dry process and allows for retention of desirable organic functionalities[1-7]. Patterning films without using any conventional lithography is economically and environmentally beneficial when it is compared to traditional lithography patterning[8-10]. In this thesis, a new approach to obtain polymer patterns is developed. This approach employs carbon nanotubes as etch masks for obtaining sub-50 nm wide polymer patterns. Carbon nanotubes are good candidates as the etching masks because of several benefits: (1) Carbon nanotubes are robust to resist oxygen plasma[11-14]. (2) Carbon nanotubes have become reasonably priced. The price of the carbon nanotubes is about $ 10 per gram. (3) The dimensions (diameter and length) of the carbon nanotubes can be controlled by growth process[15-19]. (4) Carbon nanotubes can be aligned parallel to each other on the substrate[20-32]. The functional groups on top of the patterned polymer films further enable the attachment of pre-functionalized quantum dots or nanoparticles through covalent bonding. Aligning carbon nanotubes followed by oxygen plasma etching of the underlying layer can offer new lithographic approach to fabricate polymer

patterns for further application This technique is (1) inexpensive and avoids the use of optical or electron beam assisted patterning, (2) rapid (on the order of minutes) and (3) scalable over large areas.

1.2 Initiated Chemical Vapor Deposition (iCVD)

Chemical vapor deposition (CVD) is a vacuum process that combines polymerization and coating into one single step. Traditionally, CVD is used to produce inorganic materials, such as those used in microelectronics fabrications. Initiated chemical vapor deposition (iCVD), a variation of hot filament chemical vapor deposition (HFCVD), developed in Professor Gleason's lab, is a solvent-free polymerization process [33, 34] which requires much lower energy density for deposition when it is compared to plasma-enhanced chemical vapor deposition (PECVD) (0.4-2.1 W/cm^2 [35, 36] versus 0.02-0.12 W/cm^2 [34]).

During iCVD polymerization, one initiator molecule decomposes into two free radicals via thermolysis. The iCVD polymerization is a surface controlled process [37]. The initiator free radical and monomer molecules are adsorbed onto the substrate where the surface polymerization takes place. Vinyl groups covalently anchored to a surface can react with the initiator free radicals by the same free radical polymerization mechanism responsible for polymerization of vinyl monomers.

The iCVD polymerization is a mild process and allows for retention of delicate functional groups. Poly(styrene-*alt*-maleic anhydride) deposited by iCVD is one of the examples[1, 2].

Maleic anhydride does not homopolymerize under standard free radical conditions so it must copolymerize with other monomers, such as styrene[1, 2]. Anhydride functionality can undergo acyl substitution with other nucleophilic functional group such as amine. Moreover, the iCVD polymerization provides surface coverage uniformity, conformal coatings[38], and control over film composition and surface chemistry. It is capable of producing thin films on various substrates, such as plastics, glass, and silicon wafer. Hence, iCVD permits the design of surface modification for specific applications.

1.3 Lithographic Techniques

Lithography is a patterning process used to structure materials on a fine scale. Typically, feature sizes smaller than 10 micrometers are considered to be microlithographic, and features smaller than 100 nm are referred to nanolithographic. Photolithography is one of the patterning methods, commonly applied to semiconductor manufacturing[39]. Electron beam lithography is also commercially important[40, 41]. These two conventional lithographic techniques (photolithography and electron beam lithography) will be briefly discussed and compared with some non-conventional lithographic methods.

1.3.1 Photolithography

Photolithography uses light to transfer a geometric pattern from a photomask to a light-sensitive photoresist on the substrate. The standard steps used in photolithography: (1) the substrate is covered by a photoresist. (2) a master mask is placed between the substrate and the radiation source and after exposure and development; a positive or

negative replica of the mask is reproduced on the resist. (3) the substrate material is etched or plated to obtain a patterned feature. (4) photoresist is removed by wet acid strip or dry plasma strip[39]. In a modern CMOS, a wafer will go through the photolithographic cycles up to 50 times.

The main advantage of photolithography is that it can create patterns over an entire surface simultaneously. However, the resolution limit of the feature size is limited by the diffraction limit of the wavelength of light used to illuminate the mask. Other disadvantages are that it requires a flat substrate to start with and it can require extremely clean operating conditions.

1.3.2 Electron Beam Lithography (E-beam Lithography)

E-beam lithography is the practice of scanning an electron beam in a patterned fashion across a surface covered with the resist and the patterns can be fabricated by selectively remove either exposed or non-exposed regions of the resist[40, 41].

The purpose of the e-beam lithography is to create very small structures in the resist, which can be subsequently transferred into another material for a number of purposes, for example, the creation of small electronic devices. The main advantage of e-beam lithography is that it is one of the ways to overcome the diffraction limit of light and make features in the nanometer region. For lateral structuring below the resolution limit of photolithography, e-beam lithography is a useful lithography tool.

On the other hand, the key limitation of electron beam lithography is its throughput. It takes a very long time to expose an entire substrate. The total writing time is proportional to the number of the incident electrons. A long exposure time leaves the users vulnerable to beam drift or instability. Also, since the electron beam lithography is a maskless[42] lithography, the turn-around time for reworking is lengthened unnecessarily if the pattern is not being changed the second time.

1.3.3 Non-conventional Lithography

Materials patterning through non-conventional lithography can reduce the cost of patterning structures when compared to traditional nanofabrication techniques. For example, block copolymers containing two chemically distinct chains can self assemble and phase separate into morphologies on the order of nanometer scales. Their microdomains could be lamellar, cylindrical, or spherical shapes depending on the volume fraction and inherent properties of the polymer. [8] Nanoscale patterns (< 20 nm) can be created by selectively removing one of the polymer blocks by ozonolysis, reactive ion etching or UV irradiation. [9] Nano-imprint lithography is generally low throughput and requires high temperatures/pressures, compatibility between mold and polymer. Nano-imprint lithography can achieve sub 50 nm resolution [10]. The ink jet printing allows precise deposition of polymer solutions, in which patterns form when solvent evaporates; however, feature resolution is limited by droplet size, which is about 10 μm [10].

1.4 Polymer Patterns Fabricated by Using Carbon Nanotubes as Etching Masks

Patterning functional polymers at different length scales is important for various research fields, such as semiconductor microelectronics and plastic electronics [43-45], the production of optical components such as gratings or photonic crystals [46, 47], cells and tissue engineering [48-50], and templates preparation [50, 51].

Technique based on carbon nanotubes shadow mask been reported to fabricate nanorench [11], nanogap structure and the metal junctions [12-14]. In these examples, the dimensions of the nano-structure are controlled by the structure of the carbon nanotubes. Carbon nanotubes have special dimensions and are robust to resist oxygen plasma etching process so it can act as the etch masks to fabricate polymer pattern and protect the delicate functionalities below the masks during etching process.

1.5 Quantum Dots – Properties and Application

Quantum dots (QDs) are 1-10 nm semiconductor nanocrystals with unique size-dependent optical and electrical properties due to quantum confinement [52, 53]. There are various applications of these nanocrystals in biological and environmental research, and the potential environmental and health impacts related to the use of these nanoparticles [54]. For example, quantum dots can be used at the cellular level, including immuno-labeling, cell tracking, in vivo imaging, and other related technologies [55]. Water-soluble quantum dots can be used in biomedical applications [53]. Quantum dots have several advantages of optical and chemical features over the traditional fluorescent labels [56], such as high

quantum efficiency, and long-term photostability. These features make them desirable for long-term stability and can be applied in biological system [56].

Quantum dots can be made in different colors by slightly varying size using simple, inexpensive chemical reactions, which could reduce the cost of interconnects and other structures incorporating these nanoparticles[57]. As a result of their fully quantized electronic states and high radiative efficiencies, self-assembled quantum dots can be used in a variety of novel device applications.[58] Quantum dots can function as emitters and collectors of light to transmit signals in combination with materials like carbon nanotubes or conducting polymers. Memory structures have been demonstrated based on quantum dots[59]. Quantum dots are placed inside a p-n or p-i-n diode structure, nearby or inside the depletion region. By modifying the depletion region, the memory operations (storage, writing, and erasing) are realized[59]. Each quantum dot can be used as a storage unit for the charge carriers[59].

Processes for integrating quantum dots and quantum dots assemblies into robust structures will be essential for all future technological applications[60]. In order to exploit the novel electronic and optical properties of quantum dots, fabrication methods must be developed for covalently tethering of quantum dots to surfaces with precise spatial control. Quantum dots are comprised of an inorganic nanoparticle core surrounded by organic ligands on the surface. The functional groups on the ligands can either be carboxylic acids, amines, phosphine or acrylate groups[60] and these functionalities render the quantum dots to be covalently attached to polymer patterns.

Initiated chemical vapor deposition (iCVD) of functional polymer films is an all-dry, low waste, low-energy method for achieving spatially defined tethering sites[3]. Using a patternable tethering layer is a key enabler for device fabrication. The iCVD technique can be extended to show the ability to produce functional polymer thin films and tether the functionalized quantum dots on this flexible polymer substrate.

1.6 Carbon Nanotubes Alignment

Carbon nanotubes have been studied intensely due to their unique structural, mechanical, electrical, and optical properties[61]. Carbon nanotubes are promising elements for the development of new functional nanodevices [20, 25, 61-67]. In particular, extensive effort has been made to integrate individual carbon nanotubes into microscale devices. To utilize carbon nanotubes in nanodevices, it is necessary to develop efficient strategies for their assembling into hierarchical nanostructures, which could be achieved by controlling the shape, location, and orientation of large nanotube arrays. Various methods have been proposed to pattern carbon nanotubes by using a range of principles including chemical interactions by patterned self-assembled monolayers [20, 21], physical interactions by nematic liquid crystals [22, 23], controlled flows inside a microfluidic channel [24], patterned catalytic growth [25], electric and magnetic fields [26-31], and dielectrophoretic force [32]. These methods are important for the assembly or integration of CNTs in specific environments.

The hydrodynamic flow in a micrometer scale has been demonstrated to align, position, and place both long (~2.5 m) and short (~0.8 m) carbon nanotubes by cylindrical drop

evaporating with pinned contacts[68]. Droplets of liquid drying on a surface with pinned contact area can create an internal hydrodynamic flow that carries entrained carbon nanotubes to the air-liquid-substrate interface. Individual carbon nanotubes can be aligned and placed by this top-down process. A new lithographic method to fabricate polymer patterns can be developed by combining alignment of carbon nanotube and oxygen plasma etching process. The patterned functional polymer films can be converted into different functionalities and thus can be applied in nanomaterials and nanodevice design.

Chapter 2 Experimental

2.1 Initiated Chemical Vapor Deposition (iCVD)

Figure 1 is the illustration of initiated chemical vapor deposition (iCVD) chamber. The initiator and monomers molecules were heated in this vacuum system at moderate temperature and the vapors of initiator and monomer molecules were mixed well in the channel before they entered the iCVD chamber. Each initiator molecule decomposed into two free radicals by contacting hot filaments above the substrate. This was a thermolysis process. The free radical and monomer molecules were adsorbed onto the substrate where the surface polymerization takes place. Alternative copolymers, poly(styrene-*alt*-maleic anhydride) were deposited onto silicon wafer substrate using the iCVD technique.

Poly(styrene-*alt*-maleic anhydride) was chosen since it has been known to have anhydride functionality and can undergo acyl substitution with other nucleophilic functional group such as amine. The detailed information about the design of the iCVD chamber will be described in the instrumentation section in this chapter.

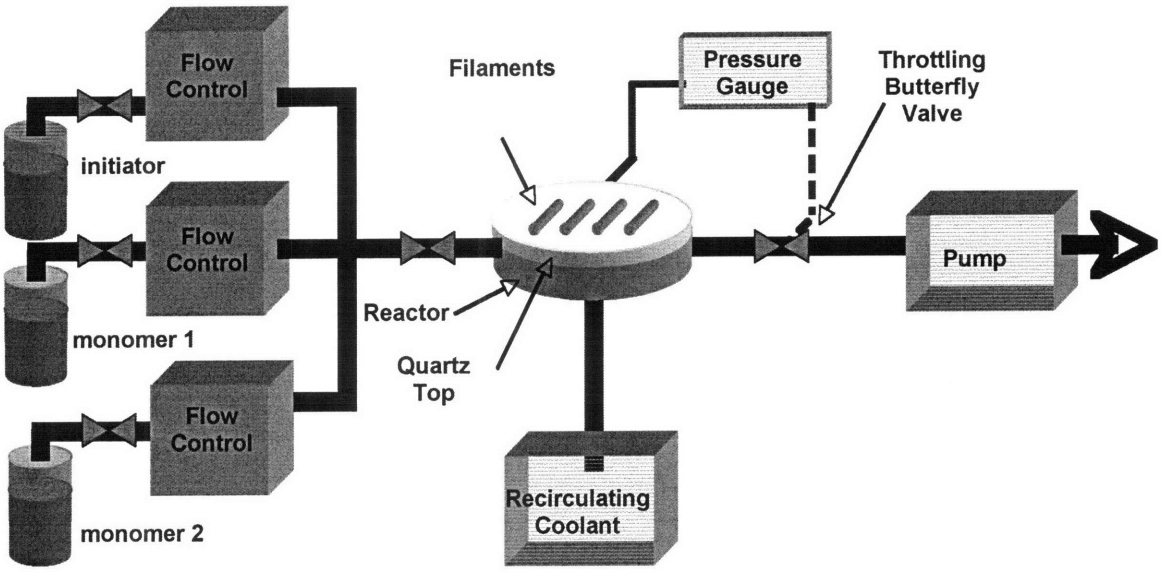

Figure 1. Illustration of the initiated chemical vapor deposition (iCVD) chamber

2.2 Functional Polymer, Poly(Styrene-*alt*-Maleic Anhydride) Synthesized via iCVD

Maleic anhydride (Ma) (99%), styrene (St) (98%), and *tert*-butyl peroxide (TBPO) (97%) were purchased from Aldrich and used for vapor phase synthesis of functional polymer thin films. They were used without further purification. Figure 2 shows the structures of monomers and polymer used in this research. Poly(styrene-alt-maleic anhydride) (PSMa) polymer thin film was deposited on the 100 mm diameter silicon (Si) wafer substrates (Wafer World) via initiated chemical vapor deposition (iCVD) as previously described[1,3]. The wafers were loaded into an iCVD chamber and then exposed to initiator and monomer vapors. The initiator, TPBO was kept in a glass jar at room temperature. Maleic anhydride and styrene molecules were heated to 90°C and 75°C respectively in a glass jar while. During iCVD, the initiators, TPBO, were decomposed by contacting hot filaments (~ 280°C) in the chamber to generates radicals and subsequently react with two monomers, styrene and maleic anhydride, by free radical polymerization. The flow rates

of maleic anhydride, styrene, TPBO remained constant at 20, 4, 4 sccm. An argon (ultrahigh purity, Airgas) patch flow was used to maintain the total flow rate at 30 sccm. $P_{Ma}/P_{Ma,sat}$ was around 0.57 while $P_{St}/P_{St,sat}$ was around 0.11. It has been proved that the compositions of this alternating copolymer are insensitive to gas feed ratios[1].

(a) Styrene (b) Maleic Anhydride (c) Poly(styrene-alt-maleic anhydride) (PSMa)

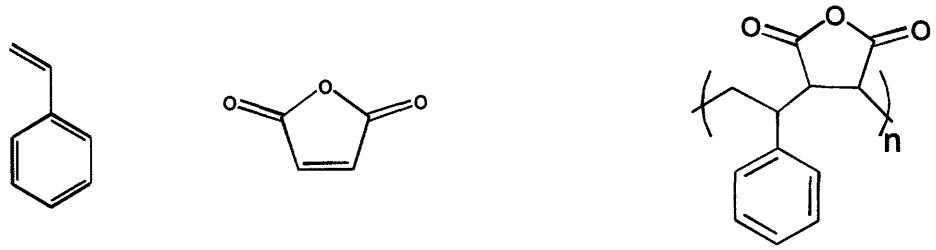

Figure 2. Structure of monomers and polymer

2.3 Polymer Patterns and Polymer/Quantum Dots Patterns

Carbon nanotubes (diameter is around 60 nm) were purchased from *Cheap Tube Inc.* Amine functionalized quantum dots, CdSe (diameter~5 nm), were purchase from Aldrich. Figure 3 shows the approach to fabricate polymer patterns on the silicon wafer: (a) Carbon nanotubes were spin-coated onto the PSMa functional polymer thin film. Carbon nanotubes were suspended in N,N-dimethylformamide (DMF) (anhydrous 99.8%, Aldrich) followed by 20 min ultrasonication. The concentration of the carbon nanotubes was less than 5 mg/L. A few drops of solution were placed on the substrates. The spinning rate for all samples was1500 rpm for 10 seconds. (b) Oxygen plasma was used to etch the functional polymer (power = 10 W). The etching time was between 10 seconds and 60 seconds. The pressure of oxygen used for plasma etching was 10 mTorr.

(The detailed information about the design of the plasma ractor will be described in the instrumentation section in this chapter.) The shape of carbon nanotubs can be transferred into the functional polymers below by etching process. (c) Carbon nanotubes were removed by rinsing it with a copious amount of water and the functional polymer patterns were obtained. (d) The amine functionalized quantum dots were incorporated into the polymer patterns. Ultrasonacation was applied before UV-Vis measurement in order to remove uncovalently attached quantum dots. The morphologies of carbon nanotubes and the polymer patterns were observed by scanning electron microscope (SEM).

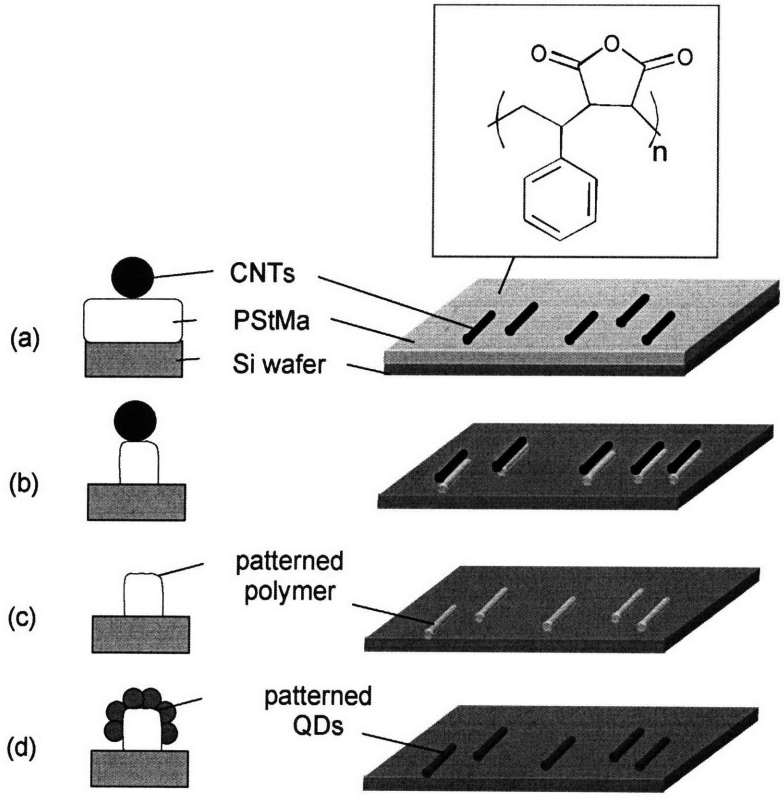

Figure 3. Approaches for fabricating polymer patterns on the silicon wafer: (a) Spin casting of CNT masks on the iCVD PSMa polymer thin film; (b) Oxygen plasma etching; (c) Removal of CNT masks; (d) Quantum dots incorporation.

2.4 CNTs Alignment Work

Single-wall carbon nanotube solution was prepared as previously described [68]. Carbon nanotubes were suspended in 1 wt % sodium dodecyl sulfate (SDS) in DI water by 10 min sonication, followed by 2-5 h centrifugation at 30 000 RPM. Different centrifugation time resulted in different concentrations of the carbon nanotube solution.

Silicon wafer were treated with oxygen plasma for 15 minutes (power = 10W) to create copious amount of hydroxyl groups. 1-hexadecylamine (HDA) molecules with long hydrocarbon chain have non-polar chain. Microcontact printing was applied by using 1-hexadecylamine (HDA) molecules as the ink (3mM) to form non-polar region on silicon wafer. Figure 4 (a) shows the chemical structure of the ink, 1-hexadecylamine (HDA) and (b) is the schematics of microcontact printing using HAD as the inks. The standard steps of microcontact printing used in this thesis: (1) the ink was applied on the stamp using a cotton swab and allowed to dry in air for 20 minutes, and (2) the stamp was placed in conformal contact with the silicon surface for about 20 minutes to transfer the pattern on to the substrate. The pattern transfer was based on the formation of hydrogen bonds between the amine groups of 1-hexadecylamine and the hydroxyl groups of the silicon wafer. The alternating polar and non-polar patterns on the substrate were prepared without rinsing any solvent.

$20\,\mu L$ of carbon nanotubes solution was drop cast on this patterned substrate having alternating rectangular polar and nonpolar areas. This film was left to dry in open air for

5 seconds, followed by rinsing with a copious amount of deionized (DI) water to remove the surfactant. The morphologies were then characterized under atomic force microscope (AFM).

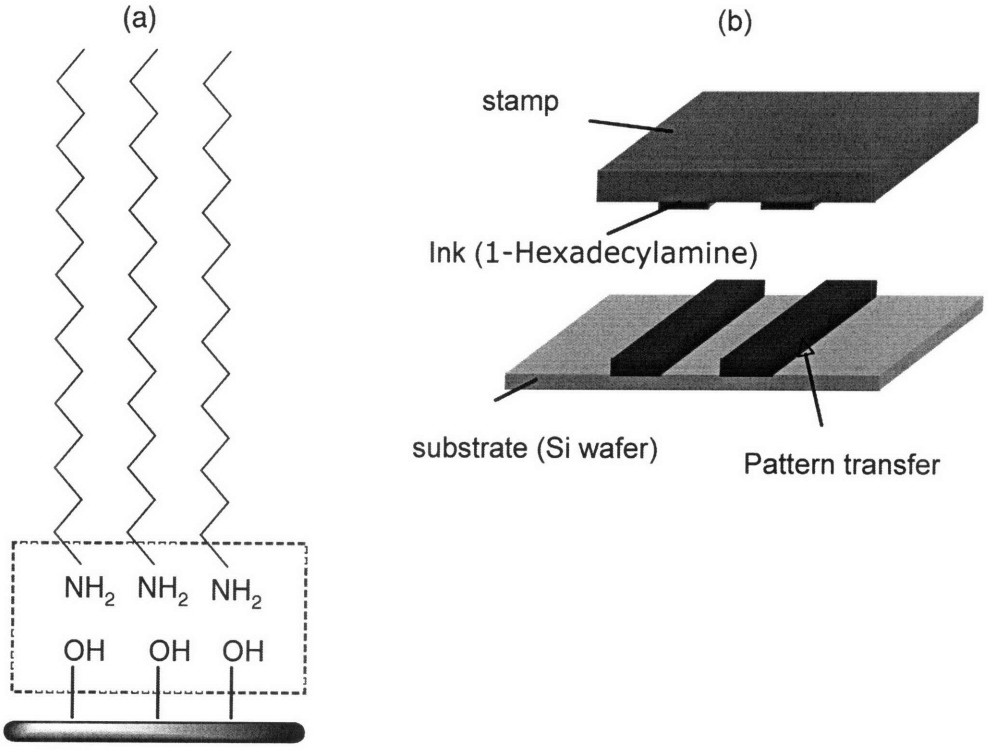

Figure 4. (a) Chemical structure of the ink, 1-hexadecylamine (HDA). (b) Schematics of microcontact printing using HAD as the inks.

2.5 Instrumentation

1) Initiated Chemical Vapor Deposition (iCVD) Chamber and Accessories

The iCVD reactor[3] was used for deposition on 100-mm-diameter Si (100) substrates. Monomer and initiator vapors were delivered into the reactor by using regulated needle valves through a port on one side of the reactor. An array of filaments (Goodfellow) were suspended over the silicon substrate at a distance and resistively heated to the

required filament temperature using a DC power supply (Sorensen). The temperature of the substrate was controlled by a circulating chiller/heater (Neslab). The pressure of the reactor was controlled by a downstream throttle valve (MKS Instruments) and a Baratron capacitance manometer (MKS Instruments). Deposition was monitored in real time by using a He-Ne laser (JDS Uniphase) that reflected off the silicon and growing film, producing an interference laser signal that cycled according to the cycle thickness of the film that was recorded as a function of time.

2) Fourier transform infrared spectroscopy (FTIR)

The Nicolet Nexus 870 ESP in 66-259 will be used for non-destructive elucidation of film composition. It contains both a liquid nitrogen cooled Mercury-Cadmium-Telluride (MCT) detector and a Deuterated Triglycine Sulfate (DTGS) detector with a KBR beam splitter.

3) Variable Angle Spectroscopic Ellipsometry (VASE)

Measurements of film thicknesses after the deposition were performed on a J. A. Woollam M-2000 spectroscopic ellipsometer. All thickness measurements were performed at a 70° incidence angle using 190 wavelengths in the range of 350-750 nm.

4) Scanning Electron Microscope (SEM)

The morphology of the carbon nanotubes and polymer patterns were observed under scanning electron microscope (JEOL 6320FV Field-Emission High-resolution SEM). The samples were coated with approximately 2 nm of gold using evaporative deposition.

It is an ultra-high-resolution scanning electron microscope capable of secondary-electron image resolution of less than 1.25 nm when operating at 15keV, and about 2.5nm when operating at 1keV.

5) UV-Visible Measurement

UV-Visible measurements were performed on DU® 800 UV/Visible Spectrophotometer over the range 400-4000 cm^{-1} in order to characterize the quantum dots.

6) Fluorescence Microscope

The fluorescence microspectroscopy (QDI 2010™ microspectrophotometer) can be used to analyze quantum dots. The sample was excited at 365 nm and the fluorescence emission was observed.

7) Optical Microscope

Optical microscopy (Olympus CX-41 microscope and Olympus TH4-100 fiber optic backlight) was used to image the structure of the microcontact printing stamps. Resolution down to 500 nm is possible.

8) O_2 Plasma Chamber

Oxygen plasma was used for O_2 plasma etching. The chamber was designed as a PECVD chamber. It is capable of treating 6" wafers with capacitive oxygen plasma. RF excitation at 13.56 MHz with 100 W maximum power.

9) Atomic Force Microscope (AFM)

The morphologies of the oriented carbon nanotubes were imaged under atomic force microscope (Veeco Metrology Nanoscope IV/Dimension 3100 Scanning Probe Microscope; tapping mode). Analysis on height images and phase images were performed to determine the position of the carbon nanotubes. Atomic force microscopy gives quantitative information on the surface roughness and feature sizes. It should be noted that atomic force microscopy does not provide accurate width information owing to the finite size of the tip. Resolution available depends on the size of the tip used, but below ~100 nm should be easily accessible. Grain size and aspect ratio measurements can be made on the AFM images.

Chapter 3 Results and Discussion

3.1 Deposition of Poly(styrene-alt-maleic anhydirde) via iCVD

Poly(styrene-alt-maleic anhydride) was deposited onto the silicon wafer in this research. Maleic anhydride is a desirable chemically reactive species because its anhydride group could be converted into different kinds of functionalities through acyl substitution reaction [69-71]. The retention of the anhydride functionality was achieved in the depositions and it can be confirmed by the presence of the double carbonyl absorption in the FTIR spectrum. FTIR bands at 1778 and 1857 cm^{-1} shown in Figure 5 are assigned to in-phase and out-of-phase stretching of the carbonyl groups in the five-membered ring of maleic anhydride.

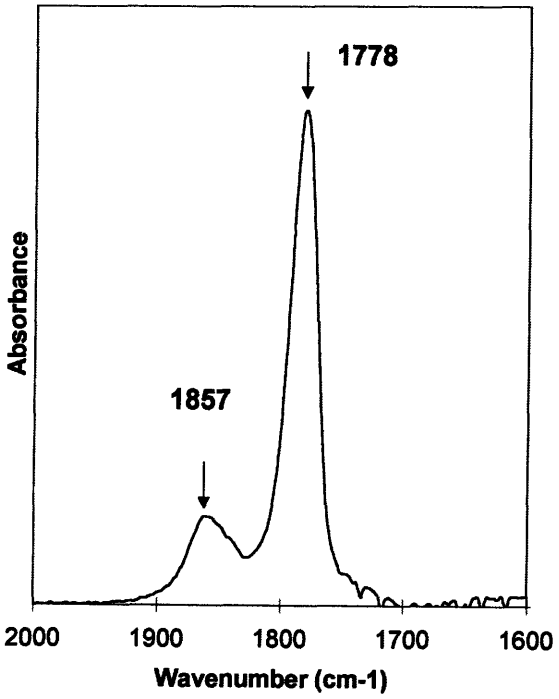

Figure 5. FTIR spectrum of the anhydride functionality of poly(styrene-alt-maleic

anhydride) thin film used in this thesis.

The copolymerization approach was chosen since it is well known that maleic anhydride does not homopolymerize under standard free radical conditions but readily copolymerizes with many monomers. Styrene was chosen as the co-monomer. The copolymer films contain 50% styrene and 50% maleic anhydride has been demonstrated by Fourier transform infrared spectroscopy, X-ray photoelectron spectroscopy, and ^{13}C nuclear magnetic resonance (NMR) as described in previous studies in Prof. Gleason's group [1-3].

3.2 Polymer Patterns Fabricated by Using Carbon Nanotubes as Etching Masks

The thickness of the film in this research was measured by spectroscopic ellipsometry. The blanket iCVD PSMa film was 20 nm in thickness. This value is smaller than the diameter of the carbon nanotube in this thesis (~60nm). Ideally, films with thicknesses less than the diameter of the carbon nanotubes are required to obtain good patterns. This is necessary to remove all the polymer in the areas which were not masked by carbon nanotubes by the isotropic etching process and obtain precise patterns.

The surface morphologies of the carbon nanotubes and the polymer patterns were characterized by SEM. The samples were coated with approximately 2 nm of gold using evaporative deposition. Figure 6 is the SEM image of the polymer substrate after spin-casting of carbon nanotubes and etching of polymer. The shapes of carbon nanotubes can

be transferred into the functional polymers below by the etching process. The diameter of the carbon nanotube was around 60 nm. No apparent change in the diameter (dimension) of the carbon nanotubes was observed from SEM images. A copious amount of waters were used to remove the carbon nanotubes. In some cases, carbon nanotubes were removed and others were not (partial removal of the carbon nanotubes). After oxygen plasma etch treatment and carbon nanotube removal, this method gave rise to polymer patterns defined by carbon nanotubes. Figure 7 shows SEM images of the polymer substrate after etching and partial removal of the carbon nanotubes. In (a), the carbon nanotube was removed, while in (b), the cabon nanotube was not. The size of the polymer pattern is smaller than the diameter of the carbon nanotubes.

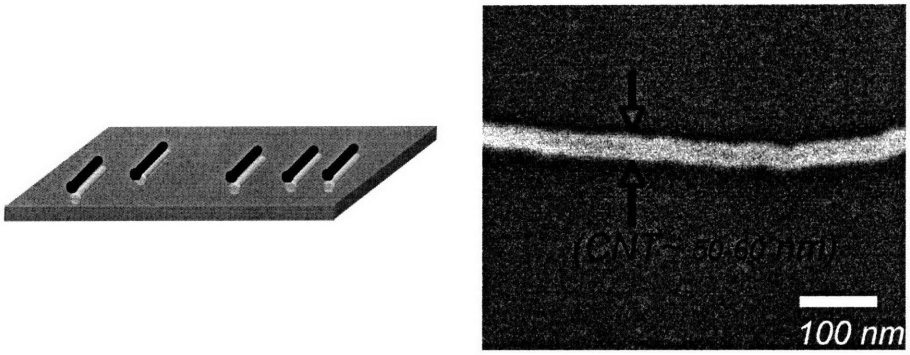

Figure 6. SEM image of the polymer substrate after spin-casting of carbon nanotubes and etching of polymer.

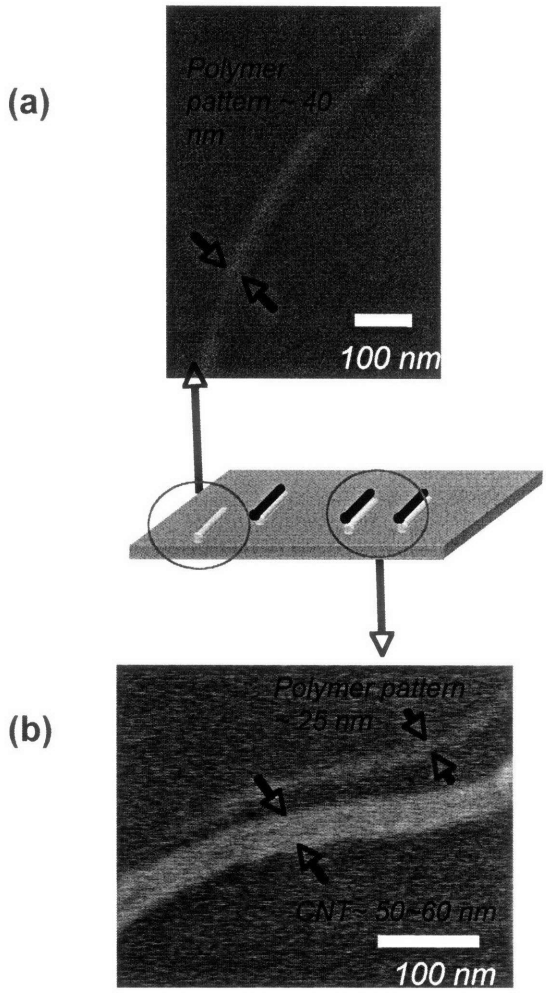

Figure 7. SEM images of the polymer substrate after etching and partial removal of the CNTs. (a) etching time was 30 sec; (b) etching time was 50 sec.

Figure 8 shows the SEM images of the polymer substrates after spin-casting of carbon nanotubes and etching of polymer. For (a) etching time was 20 sec; for (b) etching time was 30 sec; for (c) etching time was 50 sec; for (d) etching time was 60 sec. The sizes of polymer patterns are 40, 35, 25 and 20 nm, respectively. The shapes of carbon nanotubes were transferred into the functional polymers below. Etching process undercut the carbon nanotubes figure and led to a smaller polymer figure. The size of pattern polymer is smaller than the diameter of the carbon nanotube. Using different etching history, the

resolution of the polymer patterns can be down to the 20 nm. Figure 9 shows the relationship between the functional polymer pattern sizes and the etching time. It shows that the size of the patterns decreases as the etching time increases. To conclude, the pattern sizes depend on the diameters of the carbon nanotubes and the etching time.

The morphologies of the polymer patterns were fully guided by the carbon nanotubes. Several representative features of the polymer patterns, such as their shape and length, provide a straightforward indication that carbon nanotubes were directly involved in the formation of the polymer pattern. This method is a route for creating nanoscale structures with a resolution defined by the structure of the carbon nanotubes. The nanoscale dimensions, combined with the etching resistance, suggest that carbon nanotubes could be used as etching masks for nanolithography.

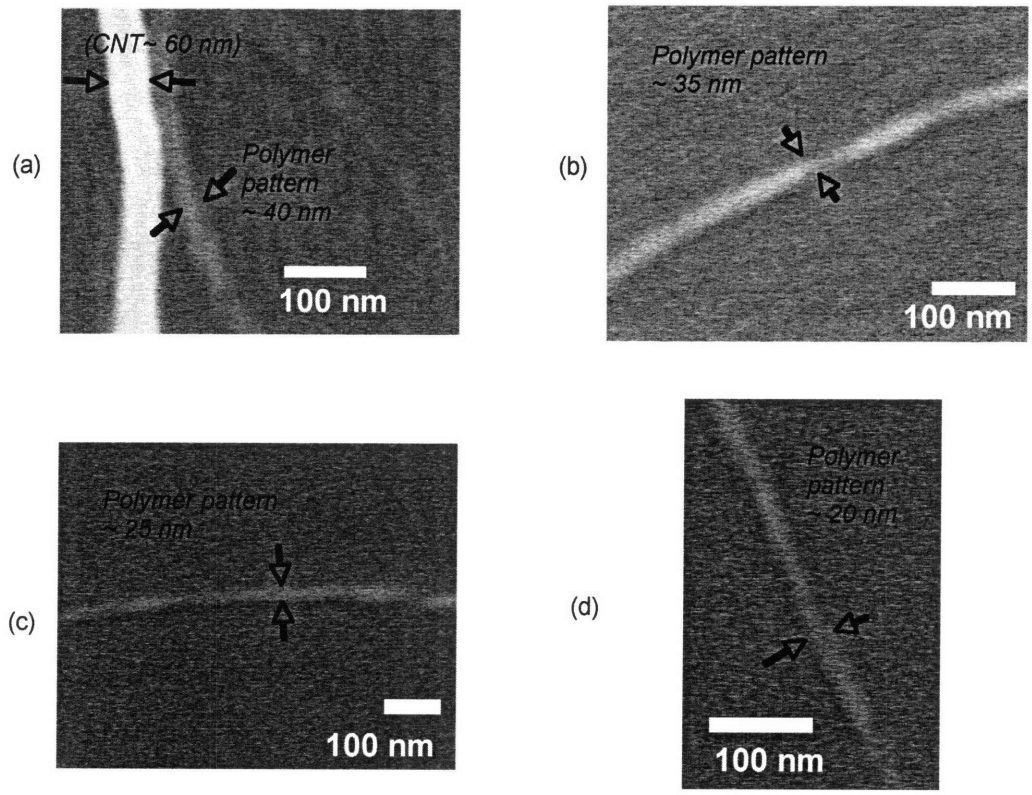

Figure 8. SEM image of the polymer substrate after etching and removal of the CNTs. (a) etching time was 20 sec; (b) etching time was 30 sec; (c) etching time was 50 sec; (d) etching time was 60 sec

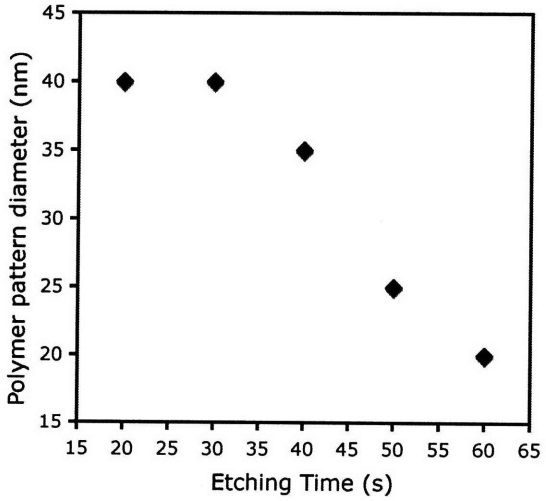

Figure 9. Relation between the functional polymer pattern sizes and the etching time

3.3 Polymer Patterns Incorporated with Quantum Dots

Functional groups in iCVD films can be used to covalently tether quantum dots. A variety of chemical functional groups can be attached to quantum dots including COOH, NH_2, and so on. Amine functionalized quantum dots CdSe were studied in this research.

The surface morphologies of the quantum dots patterns were characterized by using SEM. Figure 10 is the SEM image of the polymer pattern decorated with QDs. The crystal facets of the quantum dots were observed from this SEM images.

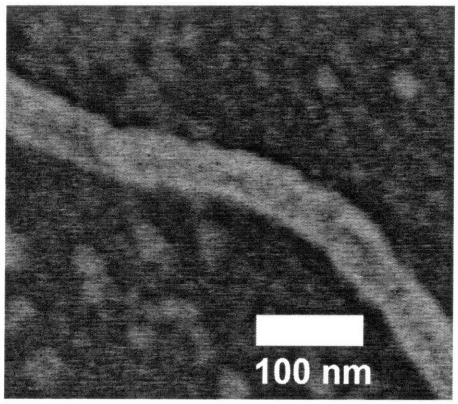

Figure 10. SEM image of the a polymer pattern after attachment of quantum dots

The UV-Vis absorption is the standard technique for assessing quantum dots. Quantum dots are active in the UV wavelength region depending on their size. UV spectra of the functional polymer (PSMa) before and after attachment of quantum dots is shown in Figure 11. The spectra of quantum dots is also shown for comparison in the Figure. Ultrasonication was applied before UV-Vis measurement in order to remove noncovalently attached quantum dots; therefore, only covalently attachment of the

quantum dots to the surface can be expected to remain. The presence of peaks at 535 and 620 nm at in the spectrum of Figure 11 confirm the successful attachment of quantum dots to the iCVD PSMa surface. A reaction mechanism was proposed for the synthesis of covalently attached CdSe quantum dots on functional polymer, PSMa using amine functionalized quantum dots and this mechanism is shown in Scheme 1.

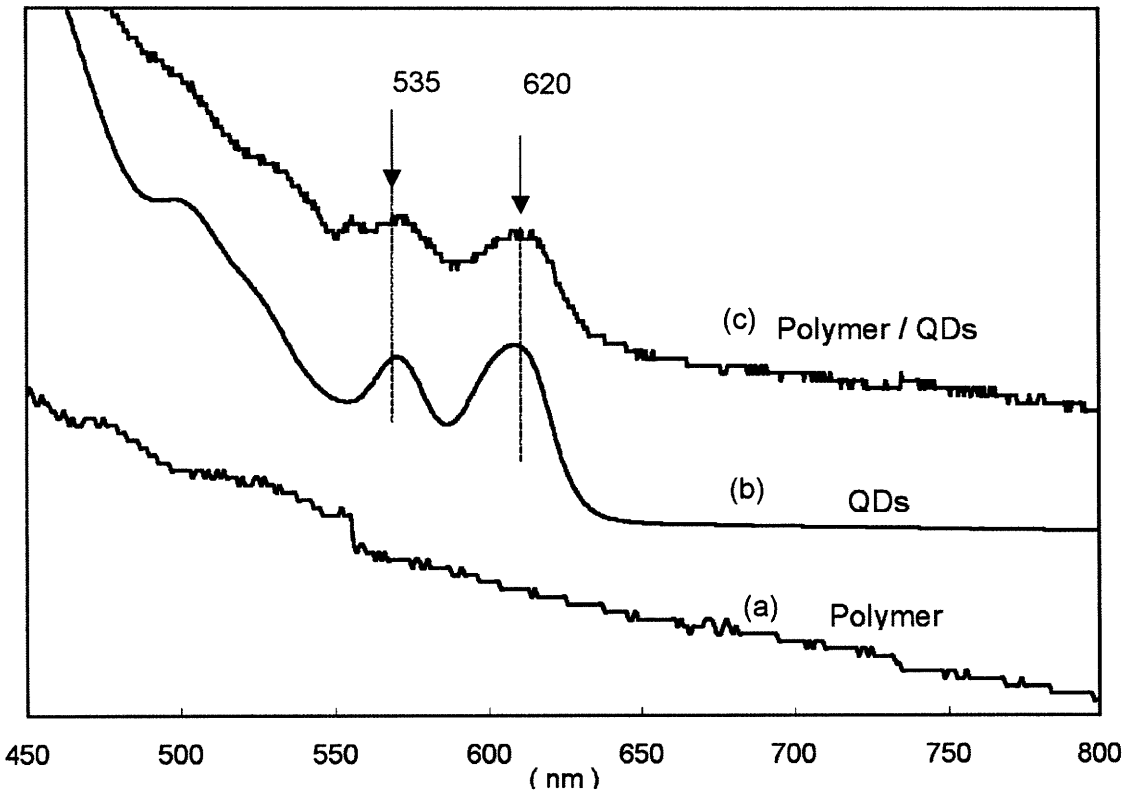

Figure 11. UV spectra of (a) functional polymer, PSMa, (b) quantum dots, CdSe, and (c) quantum dots incorporated functional polymer.

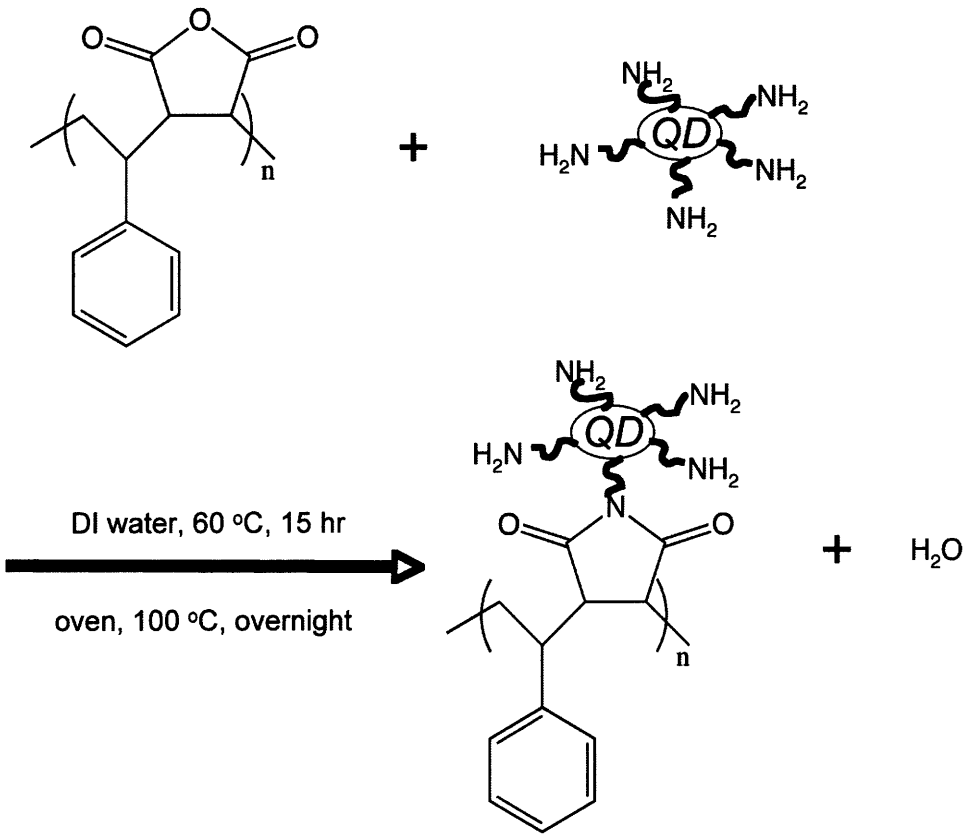

Scheme 1. Proposed reaction scheme for the synthesis of covalently attached CdSe quantum dots on functional polymer, PSMa, using amine functionalized quantum dots.

Figure 12 shows fluorescent microscope images of (a) functional polymer thin film, PSMa, (b) quantum dots (CdSe)-incorporated blanket functional polymer thin film, and (c) quantum dots (CdSe) incorporated functional polymer patterns. In (c), each florescent dot represents a bunch polymer/QD patterns. The successful attachment of quantum dots to the polymer patterns is confirmed by both UV-Visible and florescence microscope.

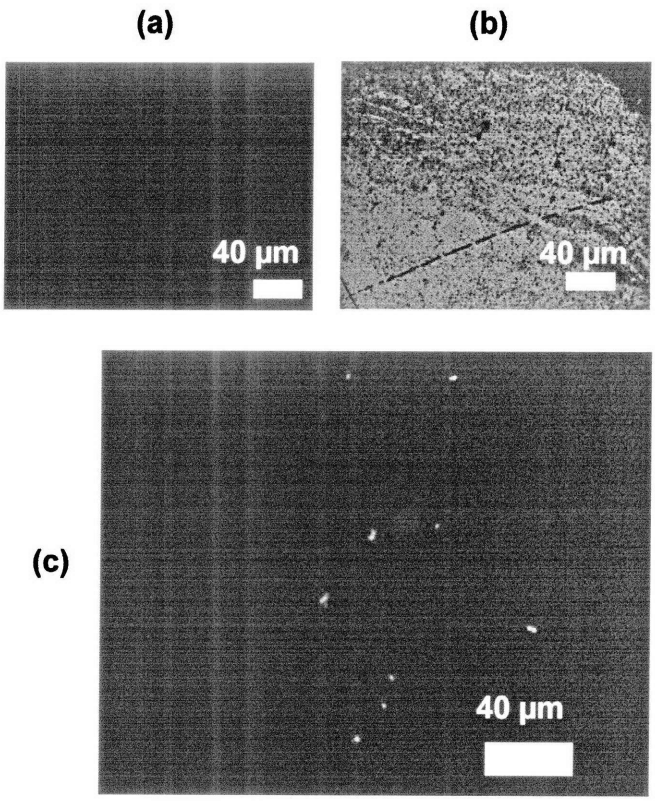

Figure 12. Fluorescent microscope images of (a) functional polymer thin film, PSMa, (b) quantum dots (CdSe) incorporated blanket functional polymer thin film, and **(c)** quantum dots (CdSe) incorporated functional polymer patterns.

A novel approach to fabricate quantum dots patterns has been established. The iCVD technology has been extended to show the ability to produce functional polymer thin films and tether the functionalized quantum dots on this flexible polymer substrate.

3.4 Carbon Nanotubes Alignment Work

Individual carbon nanotubes can be aligned and placed by the top-down process. The hydrodynamic flow in the micron scale regime has been demonstrated to place carbon nanotubes by cylindrical drop evaporating with pinned contacts[68] where the contact area is

constant with decreasing contact angle[68, 72]. Liquid evaporating near the edges is replenished by liquid from the interior because of the pinning of the contact lines of the drying drople[73-76]. Therefore, an internal flow can be developed. The pinned contact drying of droplets of particles suspensions forms "coffee ring" stains[74] due to this internal flow. All the suspended particles can be carried toward the edges of the droplet.

Figure 13 is the schematic representation of the approaches for aligning carbon nanotubes on the silicon wafer: (a) Microcontact printing was used to create rectangular non-polar areas; (b) Carbon nanotubes solution was deposited on the substrate. Initially, when carbon nanotubes solution as deposited on the surface, a thin liquid layer resulted with decreasing thickness due to evaporation. (c) The surface free energy was minimized by segregating into cylindrical droplets at a critical height of the liquid film. These cylinders were formed only in the polar region. (d) Carbon nanotubes were placed on the polar areas after the droplets dried. Rinsing with water was done to remove the surfactants.

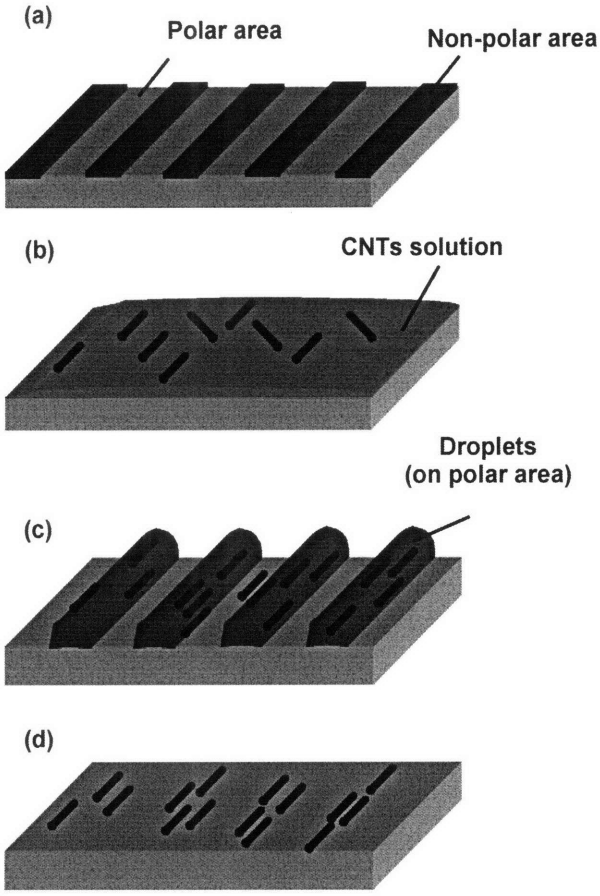

Figure 13. Schematic representation of the approaches to align the carbon nanotubes on the silicon wafer.

Figure 14 shows the optical microscopic images of the microcontact printing stamps used in this thesis. The feature size of the stamp could be investigated from this optical microscopic image. The width of the stamped area was around 3 μm.

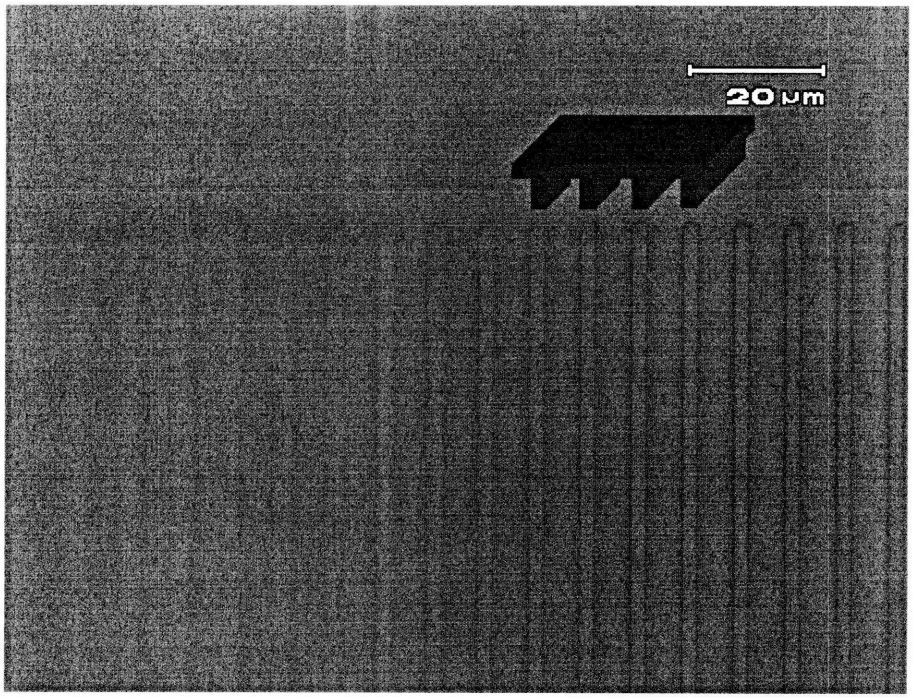

Figure 14. Optical microscopic images of the stamp.

The surface morphologies were characterized by using tapping mode atomic force microscopy (TM-AFM). Figure 15 shows the AFM image of the substrate after depositing carbon nanotubes and before rinsing the sample with a copious amount of DI water. From AFM image, we can confirm that the carbon nanotubes dispersed by surfactants were placed on the polar areas. The non-polar areas were covered by 1-hexadecylamine (HDA) molecules.

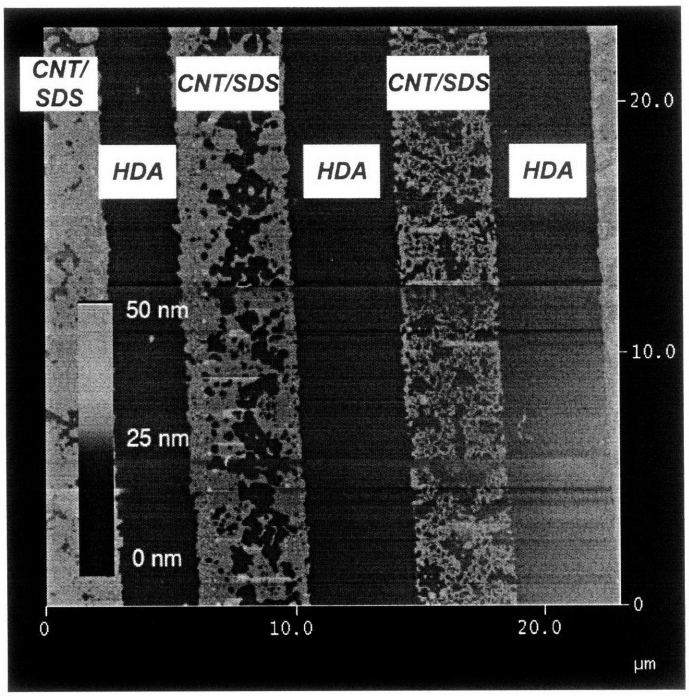

Figure 15. AFM image of the substrate after depositing carbon nanotubes dispersed by surfactants and before rinsing the sample with a copious amount of DI water.

Figure 16 to Figure 18 are the AFM images of the oriented carbon nanotubes in polar area (after removing the surfactants). The width of the polar area is around 3 μm. The height images and phase images were analyzed to determine the carbon nanotubes position. The carbon nanotubes could be highly oriented along the length of the pattern by the assistance of the hydrodynamic force.

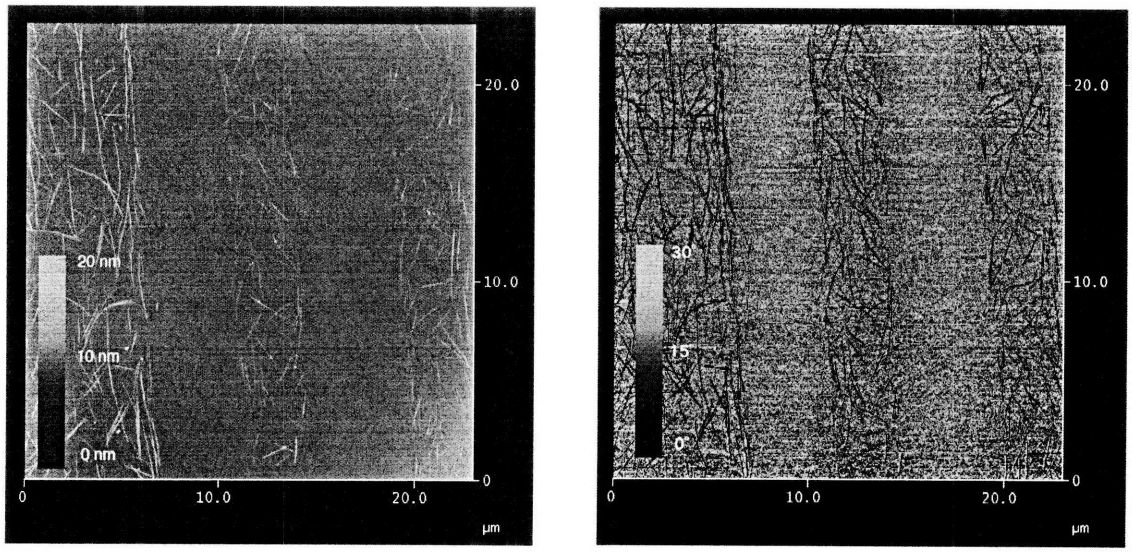

Figure 16. AFM images of oriented carbon nanotubes in polar area. (a) height image and (b) phase image.

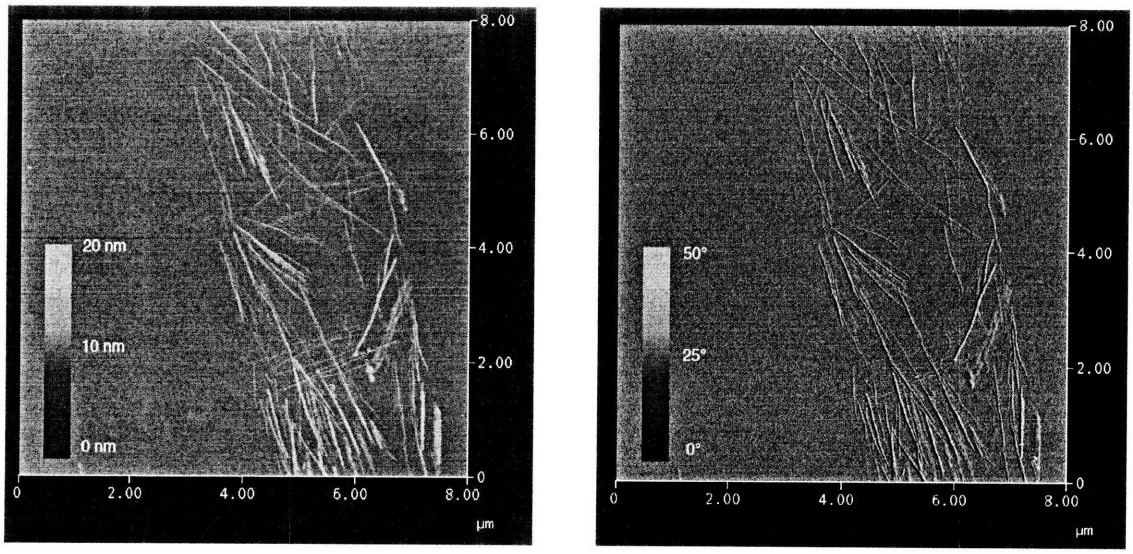

Figure 17. AFM images of oriented carbon nanotubes. (a) height image and (b) phase image.

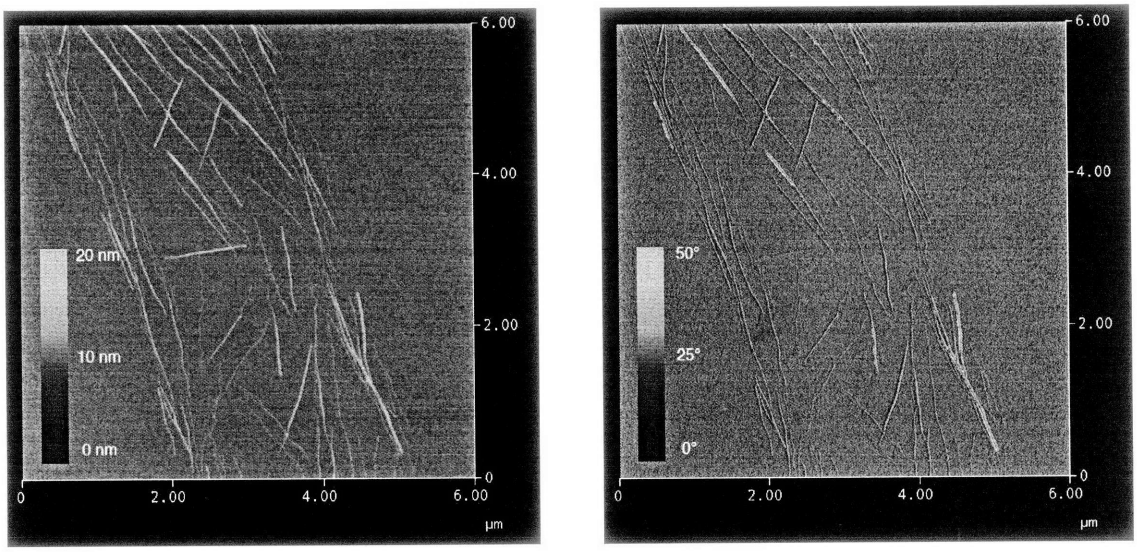

Figure 18. AFM images of oriented carbon nanotubes. (a) height image and (b) phase image.

Alignment in this research was not perfect since everything is not in parallel. The flow pattern was expected to pin the carbon nanotubes parallel to each other at the interface of the hydrophobic and the hydrophilic regions (or the edges of the hydrophilic regions). However, a lot of carbon nanotubes were observed in the hydrophilic regions. This might be due to the high evaporation rate of water. High evaporation rate of water does not leave sufficient time for the carbon nanotubes to be carried to the edges. This problem could be overcome by using a controlled environment and thereby controlling the rate of evaporation of water.

Chapter 4 Summary

Poly(styrene-*alt*-maleic anhydride) alternating copolymer thin films were deposited by using iCVD process. This benign iCVD polymerization allowed for the complete retention of the functional groups. These functional groups were further employed to tether quantum dots on the surface of the polymer films.

Sub 50 nm polymer patterns can be fabricated without using any conventional lithography. It was demonstrated successfully that carbon nanotubes could be used as etch masks for obtaining ultra-small pattern of the functionalized polymer films. Oxygen plasma etching process can be optimized without damaging the nanotube masks and the underlying functional polymer film while the unmasked polymers were removed. The shape of the patterns can be fully guided by the carbon nanotubes. The feature sizes of patterned polymer depend on the shape of the carbon nanotubes and the etching time. Features as small as 20 nm have been accomplished without using conventional lithography. Moreover, an integration method for incorporating water-soluble quantum dots onto flexible functional polymer patterns has been demonstrated.

The possibility of aligning carbon nanotubes makes this etching technique highly desirable. The hydrodynamic flow in a micrometer scale has been demonstrated to place carbon nanotubes by cylindrical drop evaporating with pinned contacts. Preliminary results showed that it is possible to align the carbon nanotubes by this method. To conclude, aligning carbon nanotubes followed by oxygen plasma etching of the

underlying layer can offer an inexpensive, rapid lithographic approach to fabricate polymer patterns for further application.

Chapter 5 Future Work

The solvent-free nature of iCVD technique can be used to coat polymers onto the substrates with a wide range of morphologies, such as non-planar surface and three-dimensional structures. Research in this direction will bring new opportunities in creating surface with peculiar properties and improving devices' performance. Also, surface graft polymerization can be done to improve stability and adhesion of the film.

Materials patterning through non-conventional lithography can reduce the cost of patterning small structures when it is compared to the traditional nanofabrication techniques, such as e-beam nanolithography and photolithography. Using carbon nanotubes as etching masks appears to be a feasible way to obtain nanoscale structures. Well-ordered nanostructure can be made for various high-density electronic components in the nanoelectronics industry by combining alignment of carbon nanotubes and oxygen plasma etching. Controllable placement of carbon nanotubes provides great potential for the device design. A number of electronic devices could be fabricated using this technique. As an example, fabrication of lines light emitting diode (LED) devices is described below: (1) Polymers patterns on P-silicon wafer can be fabricated via iCVD and the etching process. (2) The quantum dots can be attached to the polymer patterns. Heat treatment can be done to remove polymer patterns and the quantum-dot-lines can be obtained. (3) SiO_2 can be deposited as the insulator layer. (4) Gold wire can be bound onto the quantum-dot-lines. Figure 19 is the illustration of this parallel metal-semiconductor junctions.

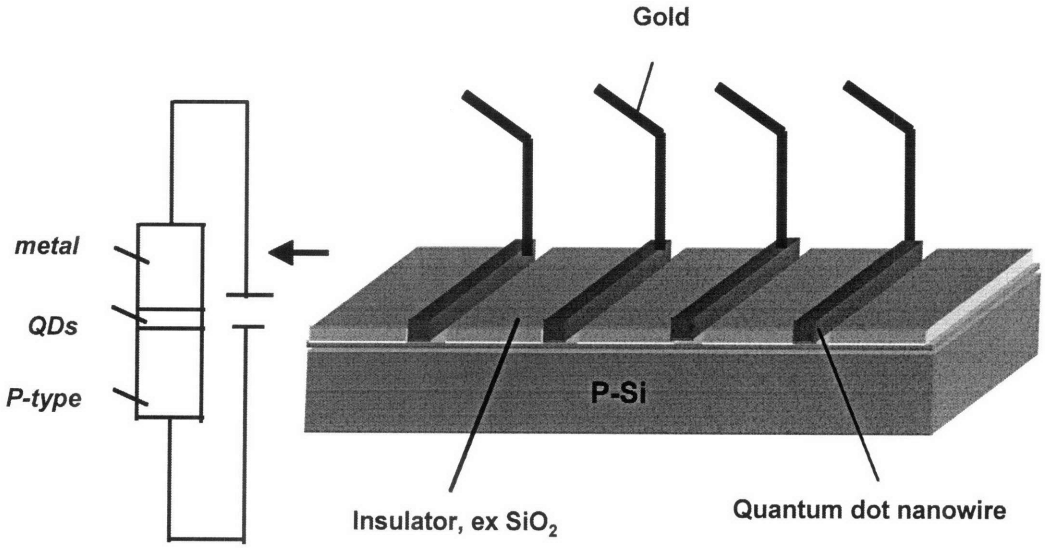

Figure 19. Illustration of parallel metal-semiconductor junctions.

References

1. Tenhaeff, W. E.; Gleason, K. K. *Langmuir* **2007,** 23, (12), 6624-6630.

2. Tenhaeff, W. E.; Gleason, K. K. *Surface & Coatings Technology* **2007,** 201, (22-23), 9417-9421.

3. Tenhaeff, W. E.; Gleason, K. K. *Advanced Functional Materials* **2008,** 18, (7), 979-992.

4. Gupta, M.; Gleason, K. K. *Langmuir* **2006,** 22, (24), 10047-10052.

5. Chan, K.; Gleason, K. K. *Langmuir* **2005,** 21, (19), 8930-8939.

6. O'Shaughnessy, W. S.; Mari-Buye, N.; Borros, S.; Gleason, K. K. *Macromolecular Rapid Communications* **2007,** 28, (18-19), 1877-1882.

7. Martin, T. P.; Kooi, S. E.; Chang, S. H.; Sedransk, K. L.; Gleason, K. K. *Biomaterials* **2007,** 28, (6), 909-915.

8. Mansky, P.; Liu, Y.; Huang, E.; Russell, T. P.; Hawker, C. *Science* **1997,** 275, (5305), 1458-1460.

9. Nagarajan, S.; Bosworth, J. K.; Ober, C. K.; Russell, T. P.; Watkins, J. J. *Chemistry of Materials* **2008,** 20, 604-606.

10. Nie, Z. H.; Kumacheva, E. *Nature Materials* **2008,** 7, (4), 277-290.

11. Byon, H. R.; Choi, H. C. *Nature Nanotechnology* **2007,** 2, (3), 162-166.

12. De Poortere, E. P.; Stormer, H. L.; Huang, L. M.; Wind, S. J.; O'Brien, S.; Huang, M.; Hone, J. *Journal of Vacuum Science & Technology B* **2006,** 24, (6), 3213-3216.

13. De Poortere, E. P.; Stormer, H. L.; Huang, L. M.; Wind, S. J.; O'Brien, S.; Huang, M.; Hone, J. *Applied Physics Letters* **2006,** 88, (14), 3.

14. Schmidt, M. S.; Nielsen, T.; Madsen, D. N.; Kristensen, A.; Boggild, P. *Nanotechnology* **2005,** 16, (6), 750-753.

15. Yoshikawa, N.; Asari, T.; Kishi, N.; Hayashi, S.; Sugai, T.; Shinohara, H. *Nanotechnology* **2008,** 19, (24), 5.

16. Pint, C. L.; Pheasant, S. T.; Pasquali, M.; Coulter, K. E.; Schmidt, H. K.; Hauge, R. H. *Nano Lett* **2008,** 8, (7), 1879-83.

17. Wang, N.; Cai, Y.; Zhang, R. Q. *Materials Science & Engineering R-Reports* **2008,** 60, (1-6), 1-51.

18. Donato, M. G.; Messina, G.; Santangelo, S. *European Physical Journal-Applied Physics* **2008,** 41, (3), 237-242.

19. Joselevich, E.; Dai, H. J.; Liu, J.; Hata, K.; Windle, A. H., Carbon nanotube synthesis and organization. In *Carbon Nanotubes*, Springer-Verlag Berlin: Berlin, 2008; Vol. 111, pp 101-164.

20. Rao, S. G.; Huang, L.; Setyawan, W.; Hong, S. H. *Nature* **2003,** 425, (6953), 36-37.

21. Wang, Y. H.; Maspoch, D.; Zou, S. L.; Schatz, G. C.; Smalley, R. E.; Mirkin, C. A. *Proceedings of the National Academy of Sciences of the United States of America* **2006,** 103, (7), 2026-2031.

22. Cervini, R.; Simon, G. P.; Ginic-Markovic, M.; Matisons, J. G.; Huynh, C.; Hawkins, S. *Nanotechnology* **2008,** 19, (17), 10.

23. van der Schoot, P.; Popa-Nita, V.; Kralj, S. *Journal of Physical Chemistry B* **2008,** 112, (15), 4512-4518.

24. Yan, Y. H.; Li, S.; Chen, L. Q.; Chan-Park, M. B.; Zhang, Q. *Nanotechnology* **2006,** 17, (22), 5696-5701.

25. Kong, J.; Soh, H. T.; Cassell, A. M.; Quate, C. F.; Dai, H. J. *Nature* **1998,** 395, (6705), 878-881.

26. Krupke, R.; Hennrich, F.; Weber, H. B.; Beckmann, D.; Hampe, O.; Malik, S.; Kappes, M. M.; Lohneysen, H. V. *Applied Physics a-Materials Science & Processing* **2003,** 76, (3), 397-400.

27. Ural, A.; Li, Y. M.; Dai, H. J. *Applied Physics Letters* **2002,** 81, (18), 3464-3466.

28. Fischer, J. E.; Zhou, W.; Vavro, J.; Llaguno, M. C.; Guthy, C.; Haggenmueller, R.; Casavant, M. J.; Walters, D. E.; Smalley, R. E. *Journal of Applied Physics* **2003,** 93, (4), 2157-2163.

29. Seemann, L.; Stemmer, A.; Naujoks, N. *Nano Letters* **2007,** 7, (10), 3007-3012.

30. Camponeschi, E.; Vance, R.; Al-Haik, M.; Garmestani, H.; Tannenbaum, R. *Carbon* **2007,** 45, (10), 2037-2046.

31. Masarapu, C.; Wei, B. Q. *Langmuir* **2007,** 23, (17), 9046-9049.

32. Chan, R. H. M.; Fung, C. K. M.; Li, W. J. *Nanotechnology* **2004,** 15, (10), S672-S677.

33. Martin, T. P.; Lau, K. K. S.; Chan, K.; Mao, Y.; Gupta, M.; O'Shaughnessy, A. S.; Gleason, K. K. *Surface & Coatings Technology* **2007,** 201, (22-23), 9400-9405.

34. Tenhaeff, W.; Gleason, K. K. *Advanced Functional Materials* **2008,** In Press.

35. Castex, A.; Favennec, L.; Jousseaume, V.; Bruat, J.; Deval, J.; Remiat, B.; Passemard, G.; Pons, M. *Microelectronic Engineering* **2005,** 82, (3-4), 416-421.

36. Wong, T. K. S.; Liu, B.; Narayanan, B.; Ligatchev, V.; Kumar, R. *Thin Solid Films* **2004,** 462, 156-160.

37. Lau, K. K. S.; Gleason, K. K. *Macromolecules* **2006,** 39, (10), 3688-3694.

38. Lau, K. K. S.; Bico, J.; Teo, K. B. K.; Chhowalla, M.; Amaratunga, G. A. J.; Milne, W. I.; McKinley, G. H.; Gleason, K. K. *Nano Letters* **2003,** 3, (12), 1701-1705.

39. del Campo, A.; Arzt, E. *Chemical Reviews* **2008,** 108, (3), 911-945.

40. Saitou, N. *International Journal of the Japan Society for Precision Engineering* **1996,** 30, (2), 107-111.

41. Takigawa, T.; Wada, H.; Ogawa, Y.; Yoshikawa, R.; Mori, I.; Abe, T. *Journal of Vacuum Science & Technology B* **1991,** 9, (6), 2981-2985.

42. Pfeiffer, H. C. *Microlithography World* **2005,** 14, (1), 4-+.

43. Shimoda, T.; Morii, K.; Seki, S.; Kiguchi, H. *Mrs Bulletin* **2003,** 28, (11), 821-827.

44. Black, C. T.; Ruiz, R.; Breyta, G.; Cheng, J. Y.; Colburn, M. E.; Guarini, K. W.; Kim, H. C.; Zhang, Y. *Ibm Journal of Research and Development* **2007,** 51, (5), 605-633.

45. Singh, T. B.; Sariciftci, N. S. *Annual Review of Materials Research* **2006,** 36, 199-230.

46. Valkama, S.; Kosonen, H.; Ruokolainen, J.; Haatainen, T.; Torkkeli, M.; Serimaa, R.; Ten Brinke, G.; Ikkala, O. *Nature Materials* **2004,** 3, (12), 872-876.

47. Campbell, M.; Sharp, D. N.; Harrison, M. T.; Denning, R. G.; Turberfield, A. J. *Nature* **2000,** 404, (6773), 53-56.

48. Thery, M.; Racine, V.; Pepin, A.; Piel, M.; Chen, Y.; Sibarita, J. B.; Bornens, M. *Nature Cell Biology* **2005,** 7, (10), 947-U29.

49. Thery, M.; Racine, V.; Piel, M.; Pepin, A.; Dimitrov, A.; Chen, Y.; Sibarita, J. B.; Bornens, M. *Proceedings of the National Academy of Sciences of the United States of America* **2006,** 103, (52), 19771-19776.

50. Kane, R. S.; Cohen, R. E.; Silbey, R. *Chemistry of Materials* **1996,** 8, (8), 1919-1924.

51. Park, M.; Harrison, C.; Chaikin, P. M.; Register, R. A.; Adamson, D. H. *Science* **1997,** 276, (5317), 1401-1404.

52. Jamieson, T.; Bakhshi, R.; Petrova, D.; Pocock, R.; Imani, M.; Seifalian, A. M. *Biomaterials* **2007,** 28, (31), 4717-4732.

53. Yu, W. W.; Chang, E.; Drezek, R.; Colvin, V. L. *Biochemical and Biophysical Research Communications* **2006,** 348, (3), 781-786.

54. Liu, W. T. *Journal of Bioscience and Bioengineering* **2006,** 102, (1), 1-7.

55. Alivisatos, A. P.; Gu, W. W.; Larabell, C. *Annual Review of Biomedical Engineering* **2005,** 7, 55-76.

56. Zhong, Y.; Kaji, N.; Tokeshi, M.; Baba, Y. *Expert Review of Proteomics* **2007,** 4, (4), 565-572.

57. Murray, C. B.; Kagan, C. R.; Bawendi, M. G. *Annual Review of Materials Science* **2000,** 30, 545-610.

58. Skolnick, M. S.; Mowbray, D. J. *Annual Review of Materials Research* **2004,** 34, 181-218.

59. Geller, M.; Marent, A.; Nowozin, T.; Bimberg, D.; Akcay, N.; Oncan, N. *Applied Physics Letters* **2008,** 92, (9), 3.

60. Bawendi, M. G.; Kim, S.; Stott, N. E. *US Patent 7160613* **2007.**

61. Baughman, R. H.; Cui, C. X.; Zakhidov, A. A.; Iqbal, Z.; Barisci, J. N.; Spinks, G. M.; Wallace, G. G.; Mazzoldi, A.; De Rossi, D.; Rinzler, A. G.; Jaschinski, O.; Roth, S.; Kertesz, M. *Science* **1999,** 284, (5418), 1340-1344.

62. Kim, P.; Baik, S.; Suh, K. Y. *Small* **2008,** 4, (1), 92-95.

63. Frank, S.; Poncharal, P.; Wang, Z. L.; de Heer, W. A. *Science* **1998,** 280, (5370), 1744-1746.

64. Hong, S. H.; Mirkin, C. A. *Science* **2000,** 288, (5472), 1808-1811.

65. Im, J.; Lee, M.; Myung, S.; Huang, L.; Rao, S. G.; Lee, D. J.; Koh, J.; Hong, S. H. *Nanotechnology* **2006,** 17, (14), 3569-3573.

66. Martel, R.; Schmidt, T.; Shea, H. R.; Hertel, T.; Avouris, P. *Applied Physics Letters* **1998,** 73, (17), 2447-2449.

67. Rueckes, T.; Kim, K.; Joselevich, E.; Tseng, G. Y.; Cheung, C. L.; Lieber, C. M. *Science* **2000,** 289, (5476), 94-97.

68. Sharma, R.; Lee, C. Y.; Choi, J. H.; Chen, K.; Strano, M. S. *Nano Letters* **2007,** 7, (9), 2693-2700.

69. Song, Z. Q.; Baker, W. E. *Journal of Polymer Science Part a-Polymer Chemistry* **1992,** 30, (8), 1589-1600.

70. Kricheldorf, H. R.; Domschke, A. *Macromolecular Chemistry and Physics* **1994,** 195, (3), 943-956.

71. Kricheldorf, H. R.; Domschke, A. *Macromolecular Chemistry and Physics* **1994,** 195, (3), 957-967.

72. Picknett, R. G.; Bexon, R. *Journal of Colloid and Interface Science* **1977,** 61, (2), 336-350.

73. Petsi, A. J.; Burganos, V. N. *Physical Review E* **2006,** 73, (4), 9.

74. Deegan, R. D.; Bakajin, O.; Dupont, T. F.; Huber, G.; Nagel, S. R.; Witten, T. A. *Nature* **1997,** 389, (6653), 827-829.

75. Petsi, A. J.; Burganos, V. N. *Physical Review E* **2005,** 72, (4), 4.

76. Deegan, R. D.; Bakajin, O.; Dupont, T. F.; Huber, G.; Nagel, S. R.; Witten, T. A. *Physical Review E* **2000,** 62, (1), 756-765.